Chemical Analysis of Lipid Boundaries after Consecutive Growth and Division of Supported Giant Vesicles

Augustin Lopez, Dimitri Fayolle, Michele Fiore, Peter Strazewski

Version of Record: https://www.sciencedirect.com/science/article/pii/S2589004220308695
Manuscript_c71c1d6f80a2ff3ce974d2c8bc5df2c0

Chemical Analysis of Lipid Boundaries after Consecutive Growth and Division of Supported Giant Vesicles†

† *in memory of Océane*

Augustin Lopez,[1] Dimitri Fayolle,[1] Michele Fiore*,[1] and Peter Strazewski[1]

[1]Université de Lyon, Université Claude Bernard Lyon 1, Institut de Chimie et Biochimie Moléculaires et Supramoléculaires, Bâtiment Edgar Lederer, 1 rue Victor Grignard, F–69622 Villeurbanne Cedex, France

Augustin Lopez (AL, augustin.lopez@etu.univ-lyon1.fr); Dimitri Fayolle (DF, dimitri.fayolle@univ-lyon1.fr); Michele Fiore (MF, michele.fiore@univ-lyon1.fr)*; Peter Strazewski (PS, strazewski@univ-lyon1.fr)

*Lead contact

Summary: The self-reproduction of giant vesicles usually results in the increase of their 'population' size. This may be achieved on giant vesicles by appropriately supplying 'mother' vesicles with membranogenic amphiphiles. The next 'generation' of 'daughter' vesicles obtained from this 'feeding' is inherently difficult to distinguish from the original mothers. Here we report on a method for the consecutive feeding with different fatty acids that each provoke membrane growth and detachment of daughter vesicles from glass microsphere-supported phospholipidic mother vesicles. We discovered that a saturated fatty acid was carried over to the next generation of mothers better than two unsaturated congeners. This has an important bearing on the growth and replication of primitive compartments at the early stages of life. Microsphere-supported vesicles are also a precise analytical tool.

Introduction. Studying the self-reproduction (Stano and Luisi, 2010; Szostak, 2017) of lipidic giant vesicles (GVs) (Walde et al., 2010) is crucial for understanding the replication of prebiotic compartments in autopoietic systems (Varela et al., 1974). This replication of shapes and objects can result from a growth and division (G&D) process: feeding the lipid boundary of a mother vesicle with amphiphilic compounds induces its growth in size and eventually its division into daughter vesicles (Fig. 1) (Stano and Luisi, 2010; Szostak, 2017). In pioneering studies, G&D of oleic acid vesicles, were carried out by feeding them with oleic anhydride that rapidly inserted into the pre-existing membranes and hydrolyzed to oleic acid and oleate at basic pH (Fig. 1A). The size of these vesicles and the G&D steps have been analyzed by microscopy (Walde et al., 1994; Wick et al., 1995). In more recent investigations, a wider variety of synthetic protocells have been used to describe the phenomenon (Lopez and Fiore, 2019; Matsuo et al., 2020, 2019; Ruiz-Mirazo et al., 2014, p.; Schwille, 2019). For instance, the observation of mother vesicles encapsulating a ferritin cargo (Berclaz et al., 2001b, 2001a) or fluorescent probes (Hanczyc et al., 2003; Zhu and Szostak, 2009) assessed their division through the distribution of their content in daughter vesicles (Fig. 1B). Furthermore, GVs composed of membranes that contained two different fluorescent probes allowed to monitor their growth in size by measuring the Förster Resonance Energy Transfer (FRET) effect (Fig. 1C) that took place when the membranes budded (Chen, 2004; Hanczyc et al., 2003). Other techniques such as free-flow electrophoresis enabled the chemical characterization of the vesicles obtained after a single self-reproduction and their sorting according to their charges (Pereira de Souza et al., 2015). However, one of the major issues in studying the G&D of GVs is the impossibility to distinguish and to separate mother from daughter vesicles after the replication step. Indeed, despite the fact that the different steps of the G&D process are

known, for instance budding, evagination, tubing, pearling, dumbell formation and division (Fig. S1), most of the lipid exchange, which actually occurs between the vesicles and the medium during the phenomenon, remains uncertain. A clear separation of mother and daughter vesicles would allow to independently characterize their lipid compositions in order to describe more precisely and reliably the lipid movements. The use of surface-mediated vesicle replication allows for the distinction of mother from daughter vesicles after a G&D process. However, only a few examples were reported in the literature. Vesicles can be anchored to a surface by either a specific integral membrane-bound linkage or through adsorption (Rebaud et al., 2014). Vesicles may be tethered to an avidin-coated surface via biotinylated phospholipids (Pignataro et al., 2000). Surface-attached vesicles would grow through the uptake of additional membrane components such as fatty acids in the form of free molecules or micelles, or through the fusion of added phospholipid vesicles. Vesicles adsorbed to a glass surface coated with hydrocarbons have also been shown to fuse with additional vesicles that were provided from a fluid flowing above. In that case, a microfluidic device delivered phospholipidic vesicles of 30–100 nm diameter that were adsorbed to and fused with the tethered lipidic quartz surface. Two-color fluorescence signatures were used to monitor the process (Johnson et al., 2002). This process was also observed by Morigaki and Walde when fatty acids micelles were delivered instead of phospholipid vesicles (Morigaki and Walde, 2002).

We have found that glass microsphere-supported giant vesicles (g-MSGVs), being GVs filled with a functionalized glass bead of a defined size (5.0 µm) bearing a tethered membrane around this glass core (schematized in Fig. 2A), can generally serve to monitor the lipids during several generations of the G&D process. We have observed that G&D arises from the budding and eventually detachment of lipid membranes that aggregate to a significant part into daughter vesicles, alike the corresponding process occurring from non-supported vesicles, commonly studied as models for protocells. (Albertsen et al., 2014; Chen, 2004; Hanczyc et al., 2003; Hardy et al., 2015; Lopez and Fiore, 2019; Terasawa et al., 2012; Tomita et al., 2011; Walde et al., 1994; Wick et al., 1995; Zhu and Szostak, 2009) Such supported membrane boundaries can be submitted to several distinct feeding processes, just as any phospholipidic vesicles can, yet with the advantage of being able to separate unambiguously the daughter vesicles formed after a G&D process from the left-over surface-supported mother vesicles by centrifugation (Fiore et al., 2018). The first preparation of this construct was reported by Gopalakrishnan et al. (Gopalakrishnan et al., 2009) by means of a mixture of phospholipids anchored to a substrate thanks, again, to an avidin/biotin interaction (Pignataro et al., 2000). G&D was performed by Monnard and co-workers who used decanoic acid/decanoate membranes supported on the same monodisperse glass bead microspheres of 5.0 µm diameter that we are presenting here (Albertsen et al., 2014). We reasoned that we could combine these separate studies to answer the question: how can the compositional dynamics during consecutive G&D processes of phospholipid boundaries be followed experimentally? Here we provide an optimization of our previously described method (Fiore et al 2018), that is, a general tool for chemically monitoring the lipid exchange that occurs during several consecutive self-reproduction processes.

One key feature of the g-MSGVs is their higher density, due to the glass bead inside, allowing for their separation by centrifugation from all lipid material floating in the host solution. Fatty acids, when supplied to g-MSGVs, partitioned into their phospholipidic boundary. This made their boundary grow in size until a fragment eventually detached to generate, among others, giant daughter vesicles (DGVs), while regularly sized supported mother vesicles with altered membrane composition were left behind. The heavier mother vesicles could be thus isolated from all lipids that detached from the mothers. The initial preparation of the g-MSGVs

covered with phospholipids (DOPC) was recently reported (Fiore et al., 2018). Phospholipids with a low critical vesicle concentration (cvc) (Zhou et al., 1999) (phospholipids **1-4**, Fig. 2B) were anchored to glass microspheres using a chemical architecture made of avidin and biotin-DSPE (**5**, Fig. 2B). The g-MSGVs were classified based on their phospholipidic composition; the list of the supported vesicles used in this study is reported in Table 1 and Table S1. POPC, DOPC, POPA and DOPA, were blended in different ratios. Pure POPC membranes were named A type, a blended binary mixture of POPC-POPA (4:1 molar ratio) B type and quaternary mixtures from POPC-POPA-DOPC-DOPA (4:1:4:1 molar ratio) C type (Tables 1 and S1). Type A^+ g-MSGVs (POPC, Table S1) containing additional 0.2 % mol/mol of DOPE-Rh (**6**, Fig. 2B) served for their observation under the confocal microscope to evidence G&D (cf. Fig. 3B). Supported vesicles containing phosphocholine extracts from soybean and egg yolk (g-MSGVs D and E, Table S1) were prepared as well. However, in order to limit the complexity of the system, these two populations of g-MSGVs bearing a tethered 'natural' membrane were not used for consecutive feeding experiments as described below. The visual aspect of the supported vesicle samples was the same whatever were their composition (Table S1, Fig. S2). Noteworthy, after the final washing step (phase 3, Fig. 2B) no floating vesicles were observed in the hosting solution (HS) (Fig. S2). Four fatty acids (**7-10**, Fig. 2B) were selected as feeding molecules. Our choice was based on the results reported by Luisi and Szostak, (Stano and Luisi, 2010; Szostak, 2017). In addition, two synthetic lipophilic and fluorescent probes ω-(dansyl)laurinyl derivative **11** and δ-(isopropanylidene)tryptophanyl derivative **12** (Schemes S1 and S2 and Figs. S16-S21) were used. The growth and partial detachment of lipid boundaries from g-MSGVs of all membrane types A-E were followed by microscopy. Due to precipitation issues with the amphiphiles **10-12** (Table 1, Entries 6-9), only oleic, myristic and myristoleic acids (**7**-**9** Fig. 2B) were kept for consecutive feeding in G&D experiments. We optimized the feeding of g-MSGVs by using ethanolic solutions of **7**-**9** at 10, 25, and 50 mM concentrations. Myristic acid (**8**) also precipitated but only when a 50 mM feeding solution was used. A 10 mM initial feeding concentration was chosen as it produced in preliminary test feedings an approximative 1:1 partitioning of the phospholipids between the first-generation g-MSGVs and the lipids in the hosting solution (Fig. S3). This 1:1 ratio was not reproduced later in more systematic tests (cf. Figs. 4, 5 and Table 1). During each feeding period ethanol evaporated only gradually, thus, it kept the fatty acids as free compounds which avoided for some time the formation of micelles or other aggregates (Walde et al., 2010). Control experiments when g-MSGVs where fed with pure ethanol showed no detachment of phospholipids in solution by microscopy (Fiore et al. 2018). The feeding ratio was tuned to 33 µL/hour and the total feeding time 3 hours. The selected parameters minimized the early de novo formation of aggregates, thus permitted to reach a total concentration of 1 mM **7**-**9** in the HS.

To stay unambiguous and clear at the same time, we renamed the g-MSGVs as g-M_nSGVs – where g- stands for glass, M stands for 'microsphere' or 'mother' and the subscript *n* is an increasing positive integer for M_1, M_2, M_3 to distinguish each mother population generated from each feeding process (Fig. 3A). The initial population of g-MSGVs was named g-M_0SGVs. With DGVs – where D stands for 'daughter' – we designated the floating vesicles generated from a first, second or third G&D process so, accordingly, an increasing subscript integer for D_1, D_2, D_3 appointed each generation of the population of daughters. With time passing after each feeding step, we observed to a varying degree the appearance of floating aggregates of lipids that accompanied the daughter vesicles. Therefore, we used the abbreviation D(GV+LA) to designate all floating lipid material in the HS, where LA stands for other lipid aggregates. After each G&D process, the supported mother vesicles g-$M_{1\text{-}3}$SGVs were isolated by sequential cycles of centrifugation and washings from all floating lipids $D_{1\text{-}3}$(GV+LA)s (Fig. 3A). In this study, we took advantage of these model giant vesicles

to independently characterize the lipid composition of the g-M_nSGVs and the D_n(GV+LA)s after every successive feeding experiment (results in Fig. 4 and Table 1). The model diagram below the images in Fig. 3B is meant as a guide that puts images taken at about the same time (1a-d) into an assumed process-dependent context. It does not imply an actual time-lapse following of the same g-MSGV in a, b, c and d. The phospholipids and fatty acids were extracted with chloroform (Bligh and Dyer, 1959). RP-HPLC (Heron et al., 2007) served to quantify the composition of fatty acids after one, two or three consecutive feeding processes (Table 1). The Stewart assay (Stewart, 1980), even if less precise than a HPLC analysis, was used to determine, independently of the fatty acid quantification, the initial (Table S2) and final (Table 1) concentration of phospholipids (PLs) in g-M_0SGVs, g-$M_{2\text{-}3}$SGVs and $D_{1\text{-}3}$(GV+LA)s, respectively. All experiments were performed in triplicate and these data were used to calculate the mean concentrations and the associated standard deviations (Table 1).

Results

Prior to any chemical analysis, we monitored that G&D was indeed occurring. The main types of phenomena described during the growth of a lipid boundary upon feeding were budding, growth (in size), pearling and division/detachment (Fig. S1) (Stano and Luisi, 2010; Szostak, 2017). They all happened upon addition of oleic, myristic and myristoleic acids (**7**-**9** Figs. 2, 3B, S8-13). Of note, there were no remarkable differences between the different coating types of g-MSGVs (A-E, Table S1) during our observations by confocal (Fig. 3B) and epifluorescence microscopy (Figs. S8-S13). However, it appeared that oleic acid (**7**) induced more easily the G&D from g-MSGVs. The critical micelle concentration (CMC) of pure **7** is 1 mM, which is lower than the CMC of shorter fatty acids—the CMC of **8** is 15 mM—and in the range of the final concentrations at the end of the feeding (0–1 mM) (Budin et al., 2012). The critical aggregation concentrations (CAC) of pure **7** and **8** are 0.1 mM and 2 mM, respectively. In our opinion, due the relatively high expected CVC of the fatty acids, and their relatively narrow pH and salt tolerance, only fatty acid micelles and aggregates were likely to form during the feeding process before they partitioned between the HS and the g-MSGV's membrane (Cape et al., 2011). Our choice for the feeding concentration and amount of added fatty acid generated final concentrations of at most 1 mM. This meant that the fraction of **7**-**9** that was not bound to the phospholipid membranes (the left-over fatty acids) could only be present in concentrations much below their respective CMC. However, the effective CAC, CMC and CVC of fatty acid mixtures may become even lower in the presence of phospholipids. Therefore, some aggregates, micelles and even vesicles could be present after the feeding period. Feeding supported giant vesicles with higher concentrations of fatty acid solutions (25 and 50 mM, Fig. S3) expectedly produced more rapidly the same previously described phenomena (Figs. S10-S12), albeit evagination was barely seen here (Fig. S1), in contrast to what we described in our previous communication (Fiore et al., 2018).

We performed a set of experiments directly above the (inverted) lens of a confocal laser scanning microscope. The prepared POPC g-M_0SGVs type A^+ membranes (Table S1) were initially expectedly spherical (Fig. 3B, image a). The formation of buds was observed after feeding g-M_0SGVs with oleic acid (25 mM ethanolic solution **7**) (Fig. 3B, image b). Such buds could increase in size during the growth step (Fig. 3B, image c). Budding and membrane growth were observed at the same moment. We noticed that, in some cases, the fast local growth also induced the formation of lipid tubes (pearling) from g-M_1SGVs, which were similar to those observed in the pearling phenomenon prior to the division of oleic acid vesicles (Fig. S1 and S13) (Szostak, 2017; Zhu et al., 2012; Zhu and Szostak, 2009). Finally, we observed the formation of new vesicles (D_1GVs, Fig. 3B, image d) due to feeding with

fatty acids. It was possible to ascertain that these new D_1GVs were freshly formed from the g-M_0SGVs, since they contained the fluorescent phospholipid probe **6** that was only added to the mother vesicles and shown not to leak even after prolonged time periods (Fig. 3B, image d). Similar observations were also made when G&D processes were performed by feeding g-M_0SGVs bearing phospholipid membranes of more complex B and C type compositions (Table S1, Figs. S8-12).

After the confirmation that G&D was indeed occurring on our mother vesicles, we set out to monitor the lipid exchange between the g-M_nSGVs and the medium during consecutive G&D. The phospholipid concentration of the g-M_0SGVs was determined by the Stewart assay using B type g-M_0SGVs (Table S1). This type of supported giant vesicles of binary compositional complexity was used as a reference for all the others, since the phospholipids (POPC and DOPC, POPA and DOPA) were fairly similar to one another (Fig. 2B). An average concentration of 0.55 mM was measured for samples containing $9 \cdot 10^5$ g-M_0SGVs. This amount corresponded to $3.7 \cdot 10^{11}$ phospholipid molecules coated on one single g-M_0SGV and compared with a maximal coating of $2 \cdot 10^8$ biotinylated tether molecules, hence, an at least 2000-fold molar excess untethered over tethered phospholipids (Table S2). Surprisingly, the amount of coated phospholipid molecules was much higher than the one expected for unilamellar vesicles (Walde et al., 2010) and can be explained by the fact that the g-MSGVs formed could be at least partly multilamellar (Albertsen et al., 2014). Besides, the multilamellarity more readily explains the pearling phenomenon (Szostak, 2017; Zhu et al., 2012; Zhu and Szostak, 2009) that was observed during the G&D from g-MSGVs (Fig. S12). The measured lipid concentrations were in general lower than expected. This was probably due to losses occurring during the extraction step. In order to compare the different conditions, the measured phospholipid concentrations were normalized to a total amount of 0.55 mM. This concentration corresponds to the initial amount present on the g-M_0SGVs in the initial sample volume before feeding started, whereas the measured fatty acid concentrations were normalized to a total concentration of 1 mM corresponding to the amount supplied during one feeding period (Fig. 4, Table 1).

The feeding of three different types of g-M_0SGV membrane coatings (A, B and C, Tables 1 and S1) was tested by performing two consecutive feedings, first with oleic acid (**7**) then myristic acid (**8**) (Fig. 4A-C, Table 1). We assumed that changing the nature of the membrane would impact the stability properties and the exchanges occurring between the g-MSGVs and the HS. Our results, instead showed that the composition of the phospholipidic membranes did not seem to have any significant impact on the feeding with fatty acids (Figs. 4A-C and 5). Of note, when the first feeding was performed using C type g-MSGVs (Fig. 4C), a higher amount of oleic acid (**7**) was found in the HS. Besides, the feeding with this fatty acid induced less detachment of phospholipids for C type g-MSGVs compared to A and B type g-MSGVs (Fig. 4A-B). The second feeding with **8** released markedly more phospholipids from C type membranes whereas the fatty acid concentrations were much the same for all types (Table 1, entries 1 and 3).

In the end, the three different populations of vesicles and floating lipid aggregates obtained, D_1(GV+LA)s, D_2(GV+LA)s and g-M_2SGVs, bore as membrane constituents a mixture of all the amphiphiles but in different molar ratios (Figs. 4A-C, 5 and Table 1). However, the amount of **7** found in the most complex C type membranes (Table 1, entry 4) was the smallest when compared to both A and B type membranes (Table 1, entries 1 and 3). We assume that this observation is related to the fact that **7** hardly exchanged with the phospholipid membrane

of the initial M_0SGVs of any membrane type A-C. In a situation where the kind of polar headgroups was constant in all types of phospholipid membranes, the difference in their acyl chains (**1**-**4**) apparently did not strongly influence the fatty acid uptake properties of the membranes.

As mentioned above, when A type g-MSGVs were first fed with oleic acid (**7**) then myristic acid (**8**), **7** was much more present in the host solution containing D_2(GV+LA)s than **8** (Fig. 4A). This result could be due to the fact that, during the second feeding, more room was available on the A type g-M_1SGVs because their phospholipids progressively detached and were released to the host solution. To test this, the order of feeding was inverted. Curiously, we observed that the concentration of myristic acid (**8**) in the HS containing D_2(GV+LA)s was still lower than that of oleic acid (**7**) (Fig. 4D). Thus, we could confirm that the saturated fatty acid **8** tended to stay more in the lipid membrane of the mother vesicles after a G&D when compared the unsaturated fatty acid **7** (Fig. 4A-D). With these experiments it was also possible to observe that the compositional complexity of a membrane could increase due to a continued feeding process because, rather than completely replacing one another, all different types of amphiphiles were present. The PC/PA headgroups (**1**-**4**), oleic and myristic acids (**7**, **8**), were found in the membranes of the second generation mother vesicles g-M_2SGVs at the end of the experiments, that is, after being separated from their D_2(GV+LA)s (Table 1).

In order to observe whether the compositional complexity could reach yet another level and if unsaturated fatty acids were indeed more released in the host solution than saturated fatty acids, a third feeding was performed with myristoleic acid (**9**, Fig. 4E). To this end, g-M_2SGVs were generated from g-M_0SGVs upon two consequent feedings with **7** and, respectively, **8** and those were supplied with **9**. After this third feeding all amphiphiles (PL = **1**, FA = **7**-**9**) were detected as constituents of, both, mothers g-M_3SGVs and daughters D_3(GV+LA)s in their respective membranes (Table 1, entry 2). Interestingly, we observed that, despite the same number of carbons present in the fatty acid chains, myristoleic acid (**9**), was more present in the host solution than myristic acid (**8**) after their respective feeding periods. Besides, after a G&D the incorporation of **9** was similar to that of **7** (oleic acid) and lower than that of **8** (Table 1). Thus, the unsaturated fatty acids **7** and **9** partitioned consistently less into the membranes of g-M_0SGVs and g-M_1SGVs after a G&D compared to the only tested saturated fatty acid **8**.

Discussion

The use of giant vesicles filled with, and supported by a monodisperse microspherical glass bead (g-MSGVs) allowed us to better understand the lipid exchange that occurred upon feeding the supported phospholipid membranes with fatty acids. For the quantification of lipid exchange we chose feeding conditions that in preliminary experiments (Fig. S3) led to the detachment of at most one half of the phospholipids from the zeroth generation mother vesicles (g-M_0SGVs) to generate membranes of daughter vesicles and some structurally less defined aggregates. We did not separately quantify the lipids that were present in giant daughter vesicles (DGVs) from those that had formed other lipid aggregates (LA), but we could identify the microscopic difference between daughter vesicles and other aggregates present in the host solution only for objects larger than about 0.5 µm. The low final feeding concentrations of the fatty acids favored their coexistence in the available phospholipid membranes and aggregates, which is consistent with the finding by others that fatty acids remain more firmly bound in phospholipid containing membranes than they would in pure fatty acid bilayer membranes (Jin et al., 2018). This paves the way for an assumed

spontaneous rigidification and enrichment of prebiotic membranes bearing higher and higher amounts of phospholipids. Pure POPC membranes and those containing 20 % POPA (coating types A and B, respectively) showed similar properties in incorporating fatty acids and detaching phospholipids (data grouped in Fig. 4F-G). Those that contained 50 % DOPC/DOPA 4:1 (C type coating) were particularly prone to be detached by myristic acid (**8**) but much less so by oleic acid (**7**) (Fig. 4H-I). In Fig. 5 the distribution of phospholipids and fatty acids in the triple-feeding experiment on A type membranes is depicted in a generation-dependent fashion, where the power of phospholipid detachment from mothers to daughters was related to the feeding material (for a more schematic graphical depiction of all distributions listed in and derived from Table 1 see Figs. S14 and S15.
We focused our attention on the mother vesicles because of their obvious superior properties as evolvable micro-compartments in later generations. The growth in size, detachment and closure of the grown membranes into giant daughter vesicles reminds very strongly of what happens when 'natural' unsupported giant vesicles grow in size then divide (G&D) into smaller daughter vesicles, thus, of vesicles that have grown in number after each feeding round and G&D process. Despite the fact that the type of membranes used for the supported vesicles did not really influence the fatty acid incorporation, we have shown that the type of fatty acid used as feeding material mattered indeed. Irrespective of the feeding order, a saturated, short fatty acid (myristic acid) was integrated in the lipid membrane of the g-MSGVs better than the unsaturated oleic and myristoleic acids.

Since both kinds, saturated and unsaturated fatty acids, were able to induce G&D, it is probable that their release from the g-M_0SGVs was different. Lately, a study using free-flow electrophoresis took advantage of the charge on deprotonated oleic acid (**7**), oleate, to show that feeding small unilamellar POPC vesicles (diameter 70 nm) with this acid led to the formation of two populations of vesicles, oleate-poor vesicles and oleate-rich vesicles (Pereira de Souza et al., 2015). Considering the fact that the same phenomena typical for G&D (budding, pearling, evagination…) have been observed on our A type first generation g-M_0SGVs (Fig. 3B, Figs. S8-S13) and regarding our results from first, second and third generation g-M_{1-3}SGVs, it is highly likely that a similar lipid exchange was occurring on our supported membranes. We have observed that more **8** was incorporated in the g-MSGV membranes than **7** whereas the amount of phospholipid released in the HS by the feeding was very similar (Figs. 4F-G and Fig 5). Thus, g-M_0SGVs made of POPC and fed with **7** would produce oleate-poor vesicles, *viz.* the g-M_1SGVs, and oleate-rich vesicles and aggregates D_1(GV+LA). Furthermore, this phenomenon would also occur when A type g-M_0SGVs were fed with myristoleic acid (**9**) (Fig. 4G, Fig 5 and Table 1). However, using a saturated fatty acid such as **8** would generate membranes that were more symmetrically blended over mothers and daughters (Figs. 4E and 5). Interestingly, 'hybrid protocells' made of these two types of amphiphiles (phospholipids and fatty acids) showed good properties of stability and permeability (Jin et al., 2018) but they also grew faster than pure fatty acid vesicles (Budin and Szostak, 2011). Our results suggest that the lipid exchange occurring on free vesicles during a G&D process are similar to the one occurring on g-MSGVs and that saturated fatty acids are the privileged amphiphilic feeding material to generate from phospholipid vesicles these more complex, more blended, thus potentially more competitive protocells (Lancet et al., 2019, 2018).

Conclusion and Perspectives

This optimized methodology for the feeding of glass microsphere-supported giant vesicles is a convenient general tool for the observation and the understanding of the growth and division

process over several feeding rounds (generations) in a more controlled analytical way than what was possible before. The method has the potential of providing experimental data for simulation studies on compositional replication in a hypothetical 'lipid world' (Kahana and Lancet, 2019; Lancet et al., 2019, 2018; Segre et al., 2000). It could also be applied to other amphiphiles and possibly tested on more artificial coatings than natural phospholipids. In the context of self-evolving compartments, the possibility of generating supported vesicles being composed of mixtures of amphiphiles opens strong perspectives for the study of vesicles that are obtained under so-called prebiotic conditions (Albertsen et al., 2014; Altamura et al., 2020; Fayolle et al., 2017; Fiore et al., 2017; Fiore and Buchet, 2020; Monnard and Deamer, 2003). In this perspective, we can now go on and test how the newly acquired fatty acids could be chemically fixed so as to enrich the compositional complexity of future generations in a more persistent way (Szostak et al., 2001).

Resource Availability

Lead Contact: michele.fiore@univ-lyon1.fr

Materials Availability. This study did generate two new unique reagents ω-(dansyl)laurinyl derivative **11** and δ-(isopropanylidene)tryptophanyl derivative **12** (Figs. S16-S22). Their chemical synthesis and characterization are described in supplementary text, and there are no restriction for availability.

Data and Code Availability. In this study, we have not used any unpublished custom code, software, or algorithm that is central to supporting the main claims of the paper.

Acknowledgments: MF wishes to dedicate this work to the memory of his beloved daughter Océane. The authors are thankful to Laura Faccin and Quentin Da Silva for their contribution in performing preliminary growth and division experiments on A type g-MSVGs. Prof. Agnès Girard-Egrot is gratefully acknowledged for her support in using the microscope facility at GEMBAS–ICMBS. The authors wish to thank Veronica La Padula of the Centre Technologique des Microstructures (CTμ) of the University Claude Bernard Lyon 1 for helping in confocal laser scanning microscopy experiments on A+ type g-M_0SGVs. MF wishes to thank professors S. Piotto (University of Salerno) and F. Rossi (University of Siena) for giving him the opportunity to present the preliminary results of this research at the congress 3rd International Conference on Bio and Nanomaterials September 29 – October 3, 2019 | MSC cruise, Mediterranean Sea. Prof. Stefano Tonzani is gratefully acknowledged for the invitation to submit this research to iScience. **Funding**: Volkswagen Foundation "Molecular Life", Az 92 850;

Author contributions: AL and MF performed all G&D experiments, HPLC analyses, Stewart assays and microscopic observations. DF and MF synthesized compounds **11** and **12**. MF conceived the project, supervised the study and wrote the first drafts of the manuscript and Electronic Supporting Information and assembled the last version of the manuscript. PS supervised the study and revised several versions of the draft manuscript. All the authors reviewed and agreed upon the submitted version of the manuscript;

Competing interests "Authors declare no competing interests."

References

Albertsen, A.N., Duffy, C.D., Sutherland, J.D., Monnard, P.-A., 2014. Self-Assembly of Phosphate Amphiphiles in Mixtures of Prebiotically Plausible Surfactants. Astrobiology 14, 462–472.

Albertsen, A. N., Maurer, S.E., Nielsen, K.A., Monnard, P.-A., 2014. Transmission of photo-catalytic function in a self-replicating chemical system: in situ amphiphile production over two protocell generations. Chem Commun 50, 8989–8992.

Altamura, E., Comte, A., D'Onofrio, A., Roussillon, C., Fayolle, D., Buchet, R., Mavelli, F., Stano, P., Fiore, M., Strazewski, P., 2020. Racemic Phospholipids for Origin of Life Studies. Symmetry 12, 1108.

Berclaz, N., Blöchliger, E., Müller, M., Luisi, P.L., 2001a. Matrix Effect of Vesicle Formation As Investigated by Cryotransmission Electron Microscopy. J. Phys. Chem. B 105, 1065–1071.

Berclaz, N., Müller, M., Walde, P., Luisi, P.L., 2001b. Growth and Transformation of Vesicles Studied by Ferritin Labeling and Cryotransmission Electron Microscopy. J. Phys. Chem. B 105, 1056–1064.

Bligh, E.G., Dyer, W.J., 1959. A rapid method of total lipid extraction and purification. Can. J. Biochem. Physiol. 37, 911–917.

Budin, I., Debnath, A., Szostak, J.W., 2012. Concentration-Driven Growth of Model Protocell Membranes. J. Am. Chem. Soc. 134, 20812–20819.

Budin, I., Szostak, J.W., 2011. Physical effects underlying the transition from primitive to modern cell membranes. Proc. Natl. Acad. Sci. 108, 5249–5254.

Cape, J.L., Monnard, P.-A., Boncella, J.M., 2011. Prebiotically relevant mixed fatty acid vesicles support anionic solute encapsulation and photochemically catalyzed trans-membrane charge transport. Chem. Sci. 2, 661.

Chen, I.A., 2004. The Emergence of Competition Between Model Protocells. Science 305, 1474–1476.

Fayolle, D., Altamura, E., D'Onofrio, A., Madanamothoo, W., Fenet, B., Mavelli, F., Buchet, R., Stano, P., Fiore, M., Strazewski, P., 2017. Crude phosphorylation mixtures containing racemic lipid amphiphiles self-assemble to give stable primitive compartments. Sci. Rep. 7, 18106.

Fiore, M., Buchet, R., 2020. Symmetry Breaking of Phospholipids. Symmetry 12, 1488.

Fiore, M., Madanamoothoo, W., Berlioz-Barbier, A., Maniti, O., Girard-Egrot, A., Buchet, R., Strazewski, P., 2017. Giant vesicles from rehydrated crude mixtures containing unexpected mixtures of amphiphiles formed under plausibly prebiotic conditions. Org. Biomol. Chem. 15, 4231–4240.

Fiore, M., Maniti, O., Girard-Egrot, A., Monnard, P.-A., Strazewski, P., 2018. Glass Microsphere-Supported Giant Vesicles for the Observation of Self-Reproduction of Lipid Boundaries. Angew. Chem. Int. Ed. 57, 282–286.

Gopalakrishnan, G., Rouiller, I., Colman, D.R., Lennox, R.B., 2009. Supported bilayers formed from different phospholipids on spherical silica substrates. Langmuir ACS J. Surf. Colloids 25, 5455–5458.

Hanczyc, M.M., Fujikawa, S., Szostak, J., 2003. Experimental Models of Primitive Cellular Compartments: Encapsulation, Growth, and Division. Science 302, 618–622.

Hardy, M.D., Yang, J., Selimkhanov, J., Cole, C.M., Tsimring, L.S., Devaraj, N.K., 2015. Self-reproducing catalyst drives repeated phospholipid synthesis and membrane growth. Proc. Natl. Acad. Sci. 112, 8187–8192.

Heron, S., Maloumbi, M.-G., Dreux, M., Verette, E., Tchapla, A., 2007. Method development for a quantitative analysis performed without any standard using an evaporative light-scattering detector. J. Chromatogr. A 1161, 152–156.

Jin, L., Kamat, N.P., Jena, S., Szostak, J.W., 2018. Fatty Acid/Phospholipid Blended Membranes: A Potential Intermediate State in Protocellular Evolution. Small 14, 1704077.

Johnson, J.M., Ha, T., Chu, S., Boxer, S.G., 2002. Early Steps of Supported Bilayer Formation Probed by Single Vesicle Fluorescence Assays. Biophys. J. 83, 3371–3379.
Kahana, A., Lancet, D., 2019. Protobiotic Systems Chemistry Analyzed by Molecular Dynamics. Life 9, 38.
Lancet, D., Zidovetzki, R., Markovitch, O., 2018. Systems protobiology: origin of life in lipid catalytic networks. J. R. Soc. Interface 15, 20180159.
Lancet, Segrè, Kahana, 2019. Twenty Years of "Lipid World": A Fertile Partnership with David Deamer. Life 9, 77.
Lopez, A., Fiore, M., 2019. Investigating Prebiotic Protocells for a Comprehensive Understanding of the Origins of Life: A Prebiotic Systems Chemistry Perspective. Life 9, 49.
Matsuo, M., Hirata, Y., Kurihara, K., Toyota, T., Miura, T., Suzuki, K., Sugawara, T., 2020. Environment-Sensitive Intelligent Self-Reproducing Artificial Cell with a Modification-Active Lipo-Deoxyribozyme. Micromachines 11, 606.
Matsuo, M., Kan, Y., Kurihara, K., Jimbo, T., Imai, M., Toyota, T., Hirata, Y., Suzuki, K., Sugawara, T., 2019. DNA Length-dependent Division of a Giant Vesicle-based Model Protocell. Sci. Rep. 9, 6916.
Monnard, P.-A., Deamer, D.W., 2003. Preparation of Vesicles from Nonphospholipid Amphiphiles, in: Methods in Enzymology. Elsevier, pp. 133–151.
Morigaki, K., Walde, P., 2002. Giant Vesicle Formation from Oleic Acid/Sodium Oleate on Glass Surfaces Induced by Adsorbed Hydrocarbon Molecules. Langmuir 18, 10509–10511.
Pereira de Souza, T., Holzer, M., Stano, P., Steiniger, F., May, S., Schubert, R., Fahr, A., Luisi, P.L., 2015. New Insights into the Growth and Transformation of Vesicles: A Free-Flow Electrophoresis Study. J. Phys. Chem. B 119, 12212–12223.
Pignataro, B., Steinem, C., Galla, H.-J., Fuchs, H., Janshoff, A., 2000. Specific Adhesion of Vesicles Monitored by Scanning Force Microscopy and Quartz Crystal Microbalance. Biophys. J. 78, 487–498.
Rebaud, S., Maniti, O., Girard-Egrot, A.P., 2014. Tethered bilayer lipid membranes (tBLMs): Interest and applications for biological membrane investigations. Biochimie 107, 135–142.
Ruiz-Mirazo, K., Briones, C., de la Escosura, A., 2014. Prebiotic Systems Chemistry: New Perspectives for the Origins of Life. Chem. Rev. 114, 285–366.
Schwille, P., 2019. Division in synthetic cells. Emerg. Top. Life Sci. ETLS20190023.
Segre, D., Ben-Eli, D., Lancet, D., 2000. Compositional genomes: Prebiotic information transfer in mutually catalytic noncovalent assemblies. Proc. Natl. Acad. Sci. 97, 4112–4117.
Stano, P., Luisi, P.L., 2010. Achievements and open questions in the self-reproduction of vesicles and synthetic minimal cells. Chem. Commun. 46, 3639.
Stewart, J.C., 1980. Colorimetric determination of phospholipids with ammonium ferrothiocyanate. Anal. Biochem. 104, 10–14.
Szostak, J.W., 2017. The Narrow Road to the Deep Past: In Search of the Chemistry of the Origin of Life. Angew. Chem. Int. Ed. 56, 11037–11043.
Szostak, J.W., Bartel, D.P., Luisi, P.L., 2001. Synthesizing life. Nature 409, 387–390.
Terasawa, H., Nishimura, K., Suzuki, H., Matsuura, T., Yomo, T., 2012. Coupling of the fusion and budding of giant phospholipid vesicles containing macromolecules. Proc. Natl. Acad. Sci. 109, 5942–5947.
Tomita, T., Sugawara, T., Wakamoto, Y., 2011. Multitude of Morphological Dynamics of Giant Multilamellar Vesicles in Regulated Nonequilibrium Environments. Langmuir 27, 10106–10112.

Varela, F.G., Maturana, H.R., Uribe, R., 1974. Autopoiesis: The organization of living systems, its characterization and a model. Biosystems 5, 187–196.
Walde, P., Cosentino, K., Engel, H., Stano, P., 2010. Giant Vesicles: Preparations and Applications. ChemBioChem 11, 848–865.
Walde, P., Wick, R., Fresta, M., Mangone, A., Luisi, P.L., 1994. Autopoietic Self-Reproduction of Fatty Acid Vesicles. J. Am. Chem. Soc. 116, 11649–11654.
Wick, R., Walde, P., Luisi, P.L., 1995. Light microscopic investigations of the autocatalytic self-reproduction of giant vesicles. J Am Chem Soc 117, 1435–1346.
Zhou, Z., Sayer, B.G., Hughes, D.W., Stark, R.E., Epand, R.M., 1999. Studies of phospholipid hydration by high-resolution magic-angle spinning nuclear magnetic resonance. Biophys. J. 76, 387–399.
Zhu, T.F., Adamala, K., Zhang, N., Szostak, J.W., 2012. Photochemically driven redox chemistry induces protocell membrane pearling and division. Proc. Natl. Acad. Sci. 109, 9828–9832.
Zhu, T.F., Szostak, J.W., 2009. Coupled Growth and Division of Model Protocell Membranes. J. Am. Chem. Soc. 131, 5705–5713.

Figure 1. Reported experiments on vesicles formed from membrane growth and/or self-reproduction processes. A) Growth and division of fatty acid (orange amphiphiles) vesicles (Walde et al., 1994; Wick et al., 1995); B) cargo distribution after growth and division (Berclaz et al., 2001b, 2001a; Hanczyc et al., 2003; Zhu and Szostak, 2009); C) vesicle growth observed by FRET (Chen, 2004; Hanczyc et al., 2003). Examples A-C do not allow for any distinction between mother and daughter vesicles; D) Tethered membranes and daughter vesicles formed by feeding glass or silica surface with fluorescent vesicles (Johnson et al., 2002; Morigaki and Walde, 2002); E) preparation of glass microsphere-supported giant phospholipid (blue amphiphiles) vesicles (Gopalakrishnan et al., 2009); F) growth and detachment of membranes using supported giant vesicles allow distinction and separation of mothers from daughters (Albertsen et al., 2014; Fiore et al., 2018).

Figure 2. Process for coating g-M_0SGVs with different phospholipids using our method and structure of used amphiphiles. A) Glass microspheres were first tethered with avidin/biotinylated phospholipid, then coated with phospholipids (Fiore et al., 2018). B) Structure of the phospholipids **1**-**6** (without counterions for clarity) used for preparation of g-M_0SGVs and fatty acids **7**-**10** used for feeding supported vesicles. Color code serves to distinguish phospholipids from fatty acids in the following figures.

Figure 3. Experimental setup and representative microscopic results. A) Workflow of monitoring of three consecutive feeding processes on phospholipid-coated glass beads, that is, glass microsphere-supported giant vesicles (g-M_0SGVs, A-C type coatings) fed with fatty acids. B) Micrographs of periodic microscopic confocal observations during feeding of POPC g-M_0SGVs bearing 0.2 % mol/mol red fluorescent DOPE-Rh (see MPB in Materials and Methods). The confocal microscope images do not correspond to a time-lapse monitoring of a single g-MSGV. They show different objects that are thought to represent the most prominent stages of a G&D model process as shown schematically below: a) A^+ type g-M_0SGVs (Table S1, entry 3) before feeding; b) budding (60 min); c) membrane growth (60 min); d) detachment with apparition of a daughter vesicle (D_1GV, 60 min). Blue arrows indicate g-M_1SGVs, white arrows the G&D phenomena and orange arrow indicates recently formed daughter vesicle. Pictures were accompanied by a simplified draw, below the confocal

images, that resume the most important phases observed during feeding experiments: The Scale bar is 5 µm for all images.

Figure 4. Graphical representation of the results as displayed in Table 1 or calculated therefrom. A-E) Concentrations (mM) of phospholipids and fatty acids in g-M_0SGVs, D_{1-3}(GVs+LA)s and g-M_{2-3}SGVs after 2 or 3 feeding periods. Composition of g-M_0SGVs: A), D), E) POPC (**1**, A type coating); B) POPC/POPA 4:1 (**1+2**, B type coating), C) POPC/POPA/DOPC/DOPA 4:1:4:1 (**1+2+3+4**, C type coating). Feeding order: A–C) first oleic acid (**7**) then myristic acid (**8**); D) first **8** then **7**; E) first **7** then **8** then myristoleic acid (**9**). F-I) Concentrations (mM) of fatty acids incorporated into g-MSGVs (F, H); phospholipids released from g-MSGVs into HS (G, I), after respective feeding periods. Amounts and standard deviations obtained from Table 1: A and B type g-MSGVs grouped (sample size = 12) (F-G); C type g-MSGVs only (sample size = 3) (H-I). Concentration of incorporated fatty acids (F, H) corresponds either to i) amount found in g-M_nSGVs if corresponding fatty acid was last supplied during feeding *n*, ii) sum of amounts found in D_{n+1}(GV+LA)s and g-M_{n+1}SGVs when corresponding fatty acid was second to last supplied during feeding *n*, iii) sum of amounts found in D_{n+1}(GV+LA)s, D_{n+2}(GV+LA)s and g-M_{n+2}SGVs when corresponding fatty acid was third to last supplied during feeding *n*. Concentration of released phospholipids (G, I) corresponds to amount found in D_n(GV+LA)s after supply with corresponding fatty acid during feeding *n*.

Figure 5. Exemplary pseudo-molecular 2D representation of triple-feeding process resulting in measured and deduced phospholipid and fatty acid concentrations and partition values (cf. Table 1, entry 2). Percentages in square brackets refer to concentration of phospholipids and fatty acids of g-M_{0-3}SGVs and D_{1-3}(GV+LA)s partitioned over A type mothers and daughters after each feeding step: [% = concentration of one amphiphile type / total concentration of this amphiphile type]. Total concentration of PL (0.55 mM, 215 blue objects) corresponds to amount on g-M_0SGVs. Total concentration of each fatty acid (1 mM, 390 yellow, green or red objects) corresponds to supply during each respective feeding period. Object sizes not scaled, number of tethered molecules not proportional, multilamellarity not depicted.

Table 1. Microscopic and chemical analysis of lipid boundaries content after two or three consecutive feeding experiments on D_1(GV+LA)s, D_2(GV+LA)s, D_3(GV+LA)s, g-M_2SGVs and g-M_3SGVs by using g-M_0SGVs type A-C (for the full data set see Tables S1-S2).

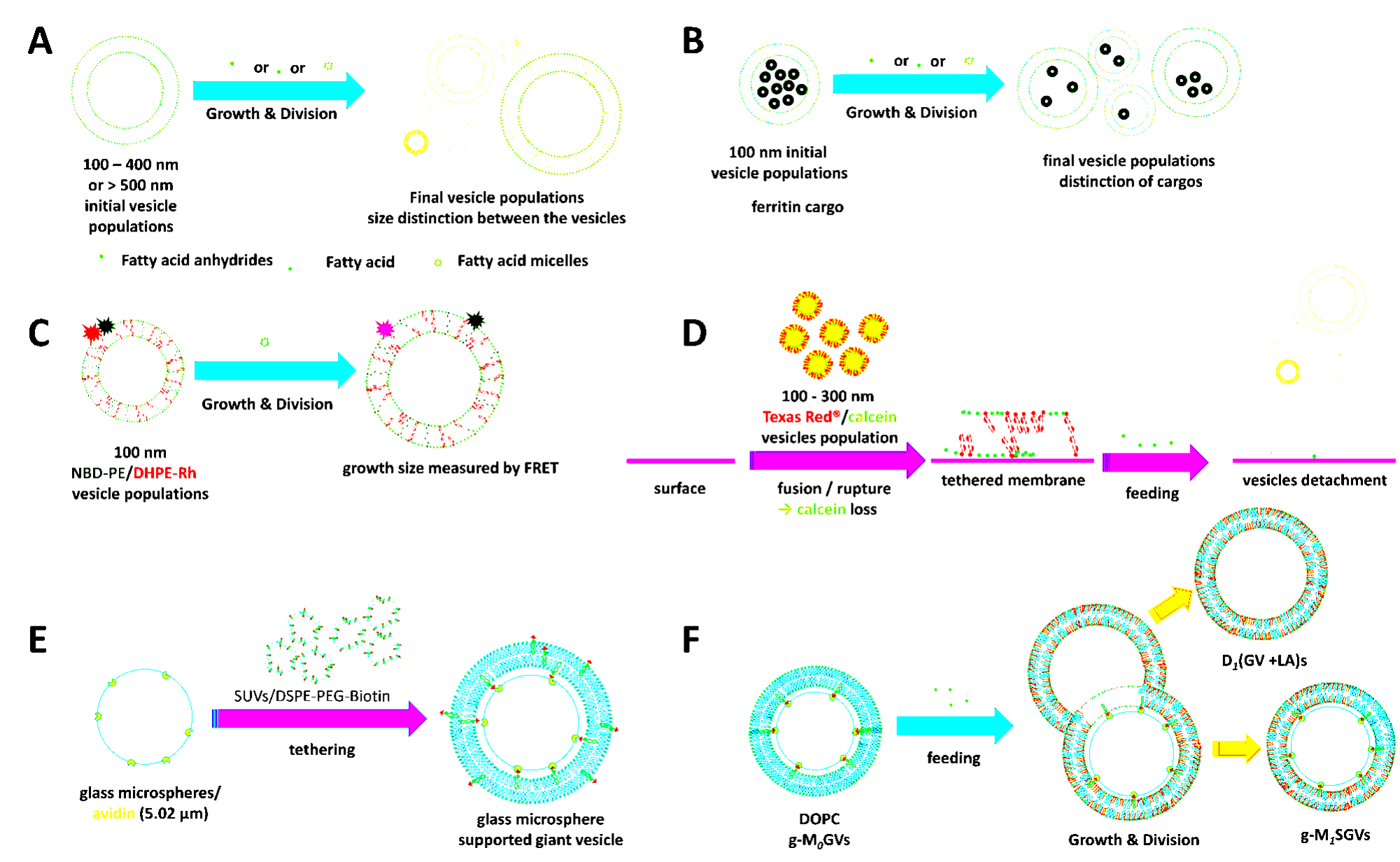
A
or or
Growth & Division
100 – 400 nm
or > 500 nm
initial vesicle
populations
Final vesicle populations
size distinction between the vesicles
Fatty acid anhydrides
Fatty acid
Fatty acid micelles
B
or or
Growth & Division
100 nm initial
vesicle populations
ferritin cargo
final vesicle populations
distinction of cargos
C
Growth & Division
100 nm
NBD-PE/DHPE-Rh
vesicle populations
growth size measured by FRET
D
100 - 300 nm
Texas Red®/calcein
vesicles population
surface
fusion / rupture
→ calcein loss
tethered membrane
feeding
vesicles detachment
E
SUVs/DSPE-PEG-Biotin
tethering
glass microspheres/
avidin (5.02 µm)
glass microsphere
supported giant vesicle
F
feeding
DOPC
g-M0GVs
D1(GV +LA)s
Growth & Division
g-M1SGVs

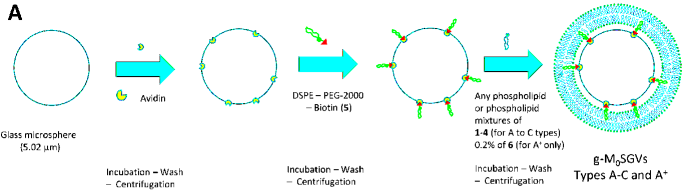
A
Glass microsphere
(5.02 μm)
Avidin
Incubation – Wash
– Centrifugation
DSPE – PEG-2000
– Biotin (5)
Incubation – Wash
– Centrifugation
Any phospholipid
or phospholipid
mixtures of
1-4 (for A to C types)
0.2% of 6 (for A+ only)
Incubation – Wash
– Centrifugation
g-M0SGVs
Types A-C and A+

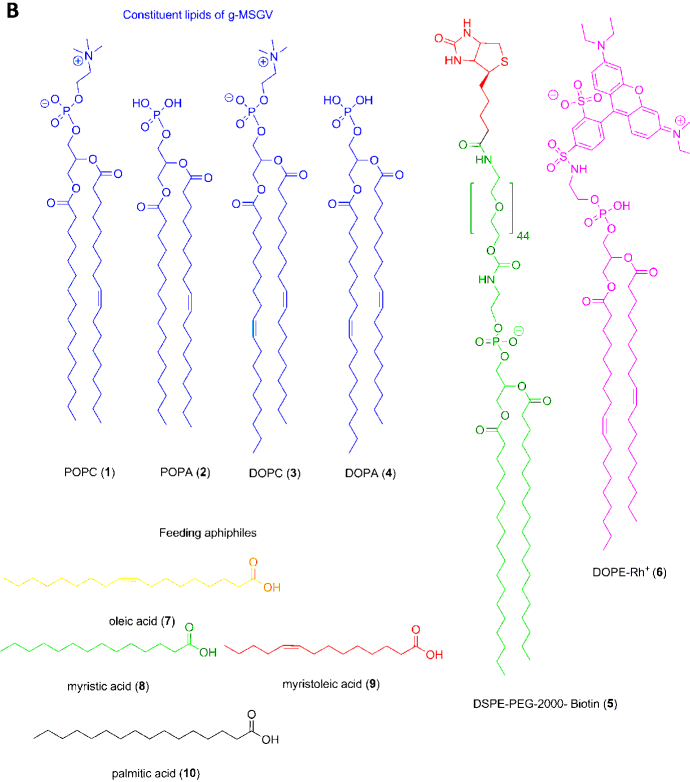
B
Constituent lipids of g-MSGV
POPC (1)
POPA (2)
DOPC (3)
DOPA (4)
DSPE-PEG-2000- Biotin (5)
DOPE-Rh+ (6)
Feeding aphiphiles
oleic acid (7)
myristic acid (8)
myristoleic acid (9)
palmitic acid (10)

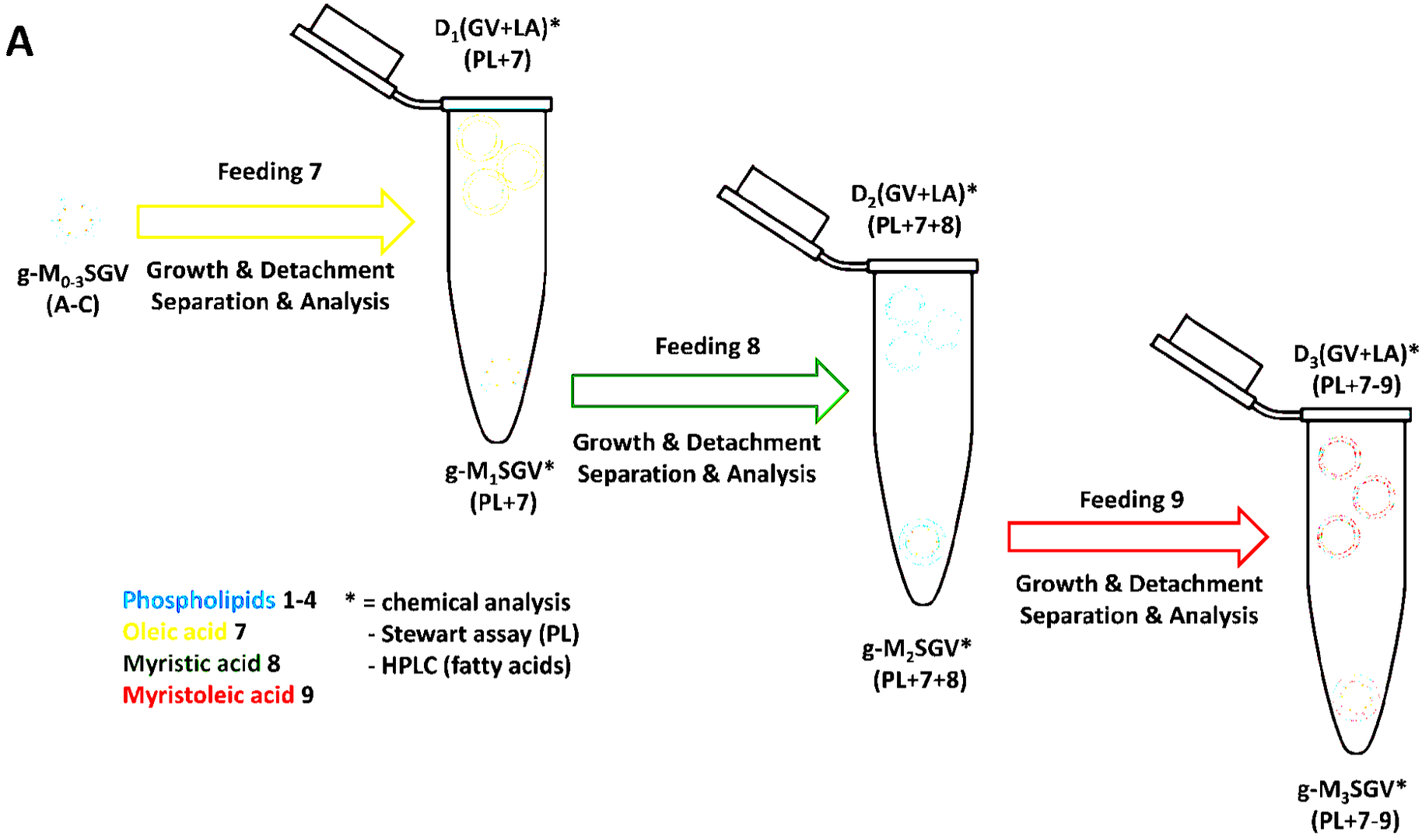
A
D1(GV+LA)*
(PL+7)
Feeding 7
g-M0-3SGV
(A-C)
Growth & Detachment
Separation & Analysis
g-M1SGV*
(PL+7)
D2(GV+LA)*
(PL+7+8)
Feeding 8
Growth & Detachment
Separation & Analysis
g-M2SGV*
(PL+7+8)
D3(GV+LA)*
(PL+7-9)
Feeding 9
Growth & Detachment
Separation & Analysis
g-M3SGV*
(PL+7-9)
Phospholipids 1-4
Oleic acid 7
Myristic acid 8
Myristoleic acid 9
* = chemical analysis
- Stewart assay (PL)
- HPLC (fatty acids)

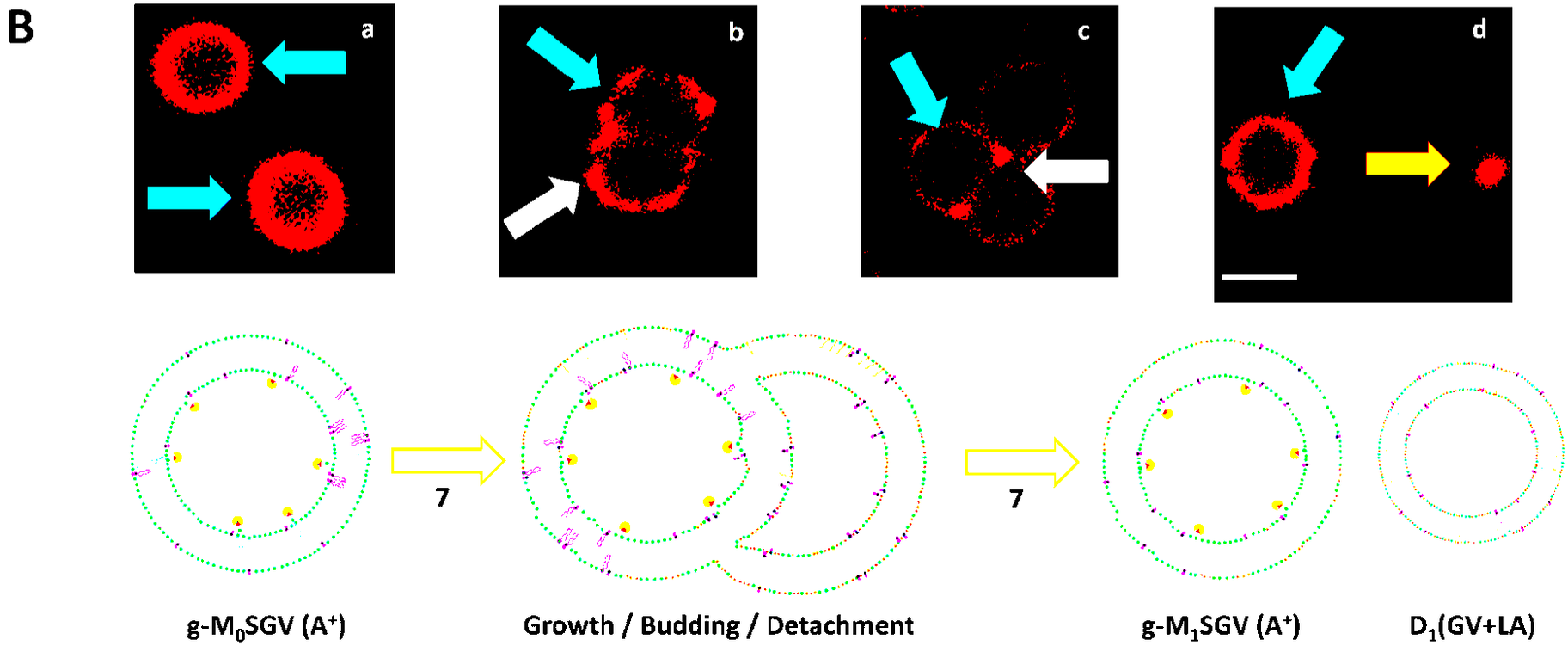
B
a
b
c
d
7
7
g-M0SGV (A+)
Growth / Budding / Detachment
g-M1SGV (A+)
D1(GV+LA)

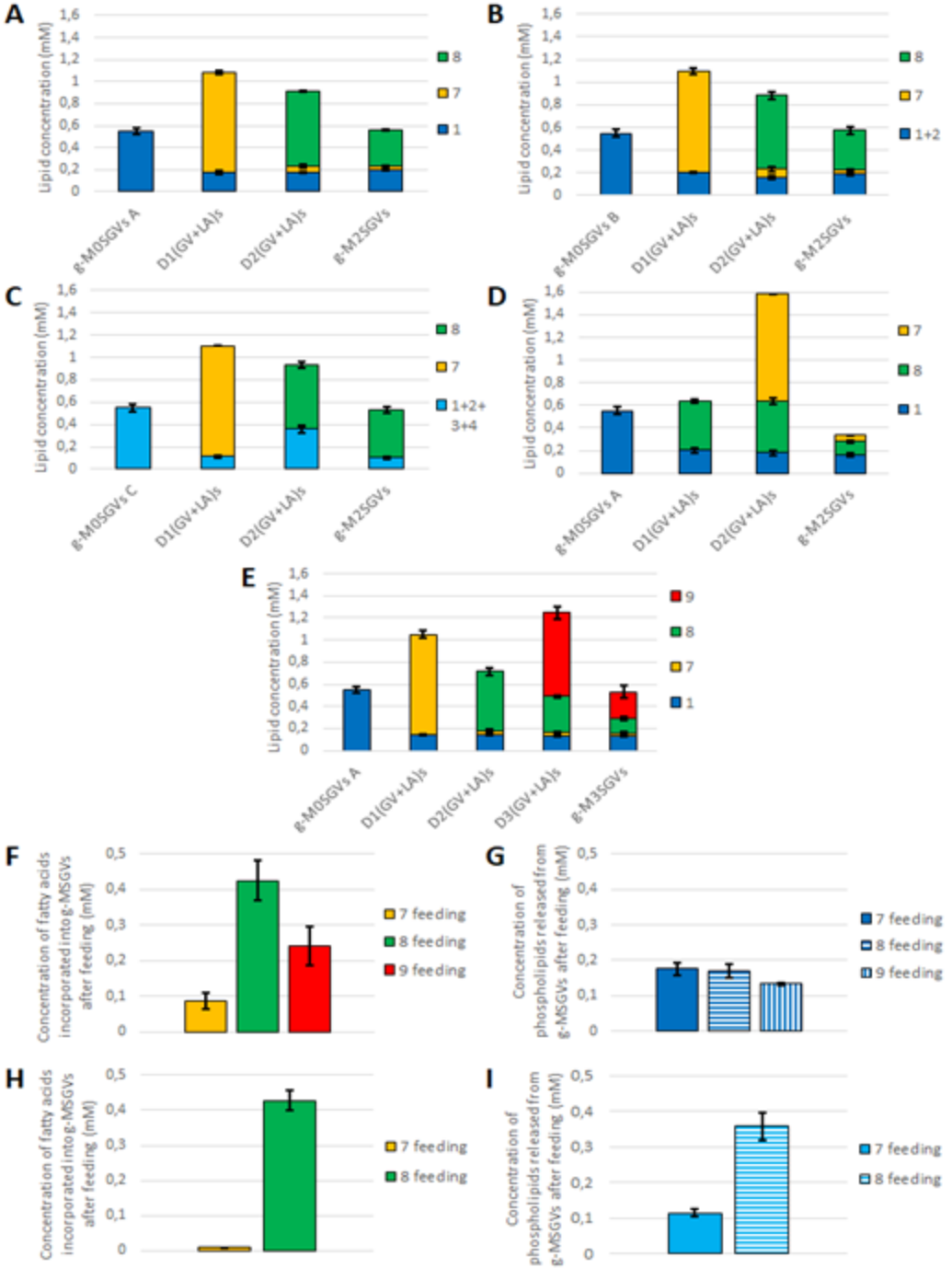
A
Lipid concentration (mM)
1,6
1,4
1,2
1
0,8
0,6
0,4
0,2
0
8
7
1
g-M05GVs A
D1(GV+LA)s
D2(GV+LA)s
g-M25GVs
B
Lipid concentration (mM)
8
7
1+2
g-M05GVs B
D1(GV+LA)s
D2(GV+LA)s
g-M25GVs
C
Lipid concentration (mM)
8
7
1+2+ 3+4
g-M05GVs C
D1(GV+LA)s
D2(GV+LA)s
g-M25GVs
D
Lipid concentration (mM)
7
8
1
g-M05GVs A
D1(GV+LA)s
D2(GV+LA)s
g-M25GVs
E
Lipid concentration (mM)
9
8
7
1
g-M05GVs A
D1(GV+LA)s
D2(GV+LA)s
D3(GV+LA)s
g-M35GVs
F
Concentration of fatty acids incorporated into g-MSGVs after feeding (mM)
0,5
0,4
0,3
0,2
0,1
0
7 feeding
8 feeding
9 feeding
G
Concentration of phospholipids released from g-MSGVs after feeding (mM)
0,5
0,4
0,3
0,2
0,1
0
7 feeding
8 feeding
9 feeding
H
Concentration of fatty acids incorporated into g-MSGVs after feeding (mM)
0,5
0,4
0,3
0,2
0,1
0
7 feeding
8 feeding
I
Concentration of phospholipids released from g-MSGVs after feeding (mM)
0,5
0,4
0,3
0,2
0,1
0
7 feeding
8 feeding

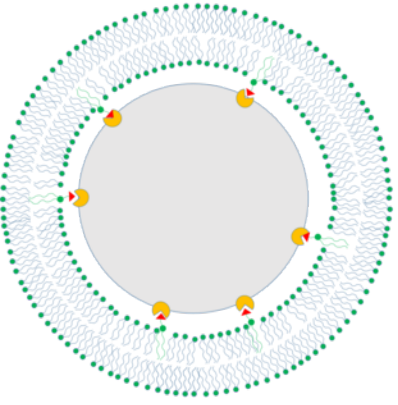

g-M$_1$SGV A

PL **1**: 0.55 mM [100%]

Feeding with **7**:
1 mM [100%]

1st G & D

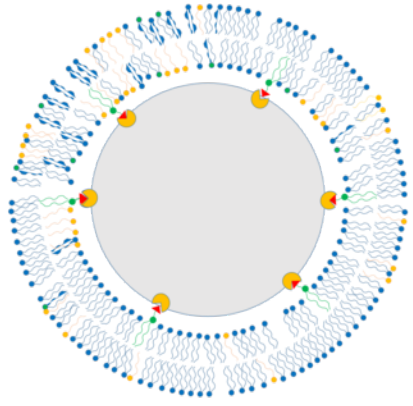

g-M$_1$SGV A

Left-over **PL**: 0.41 mM [75%]
Incorporated **7**: 0.09 mM [9%]

into HS

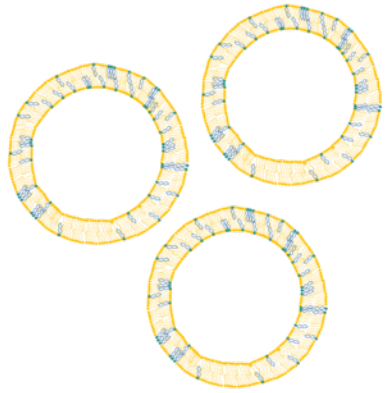

D$_1$(GV+LA)s

Detached **PL**: 0.14 mM [25%]
Left-over **7**: 0.91 mM [91%]

Feeding with **8**:
1 mM [100%]

2nd G & D

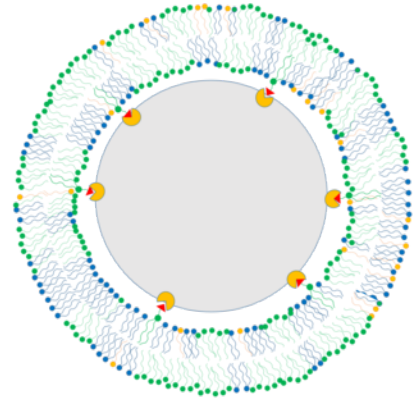

g-M$_2$SGV A

Left-over **PL**: 0.26 mM [48%]
Left-over **7**: 0.06 mM [6%]
Incorporated **8**: 0.46 mM [46%]

Into HS

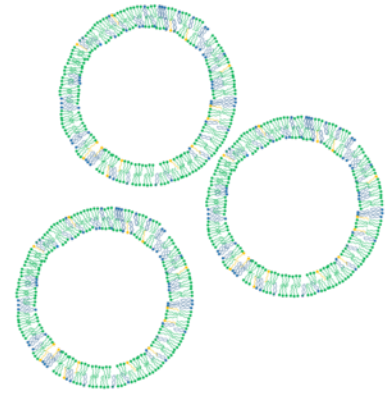

D$_2$(GV+LA)s

Detached **PL**: 0.15 mM [27%]
Detached **7**: 0.03 mM [3%]
Left-over **8**: 0.54 mM [54%]

Feeding with **9**:
1 mM [100%]

3rd G & D

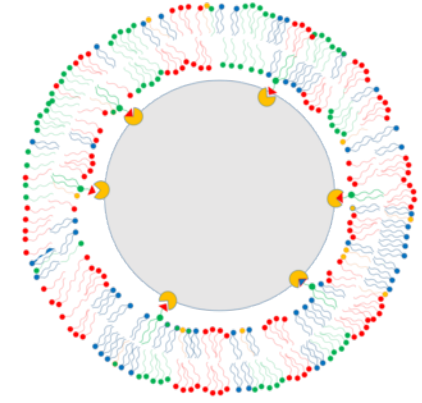

g-M$_3$SGV A

Left-over **PL**: 0.13 mM [24%]
Left-over **7**: 0.03 mM [3%]
Left-over **8**: 0.13 mM [13%]
Incorporated **9**: 0.24 mM [24%]

Into HS

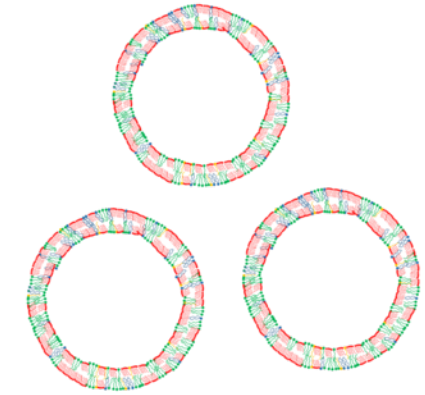

D$_3$(GV+LA)s

Detached **PL**: 0.13 mM (24%)
Detached **7**: 0.03 mM [3%]
Detached **8**: 0.33 mM [33%]
Left-over **9**: 0.76 mM [76%]

						1st feeding	2nd feeding	3rd feeding	
Entry	g-M_0SGVs[a]	Microscopic observations[b]	Vesicles product	PL conc. [c,d] (mM)	PL_{found} / $PL_{initial}$	**7** $_{found}$/**7** $_{fed}$ [d],[e]	**8** $_{found}$/**8** $_{fed}$ [d],[e]	**9** $_{found}$/**9** $_{fed}$ [d],[e]	Final composition
1	A (**1**)	Budding, Growth, Pearling and Division	D_1(GV+LA)s	0 18 ± 0.01	0.33 ± 0.01	0.90 ± 0.01	-	-	**1+7**
			D_2(GV+LA)s	0.17 ± 0.01	0.31 ± 0.01	0.06 ± 0.02	0.68 ± 0.01	-	**1+7+8**
			g-M_2SGVs	0.20 ± 0.01	0.36 ± 0.01	0.04 ± 0.01	0.32 ± 0.01	-	**1+7+8**
2	A (**1**)	Budding, Growth, Pearling and Division	D_1(GV+LA)s	0.14 ± 0.01	0.25 ± 0.01	0.91 ± 0.03	-	-	**1+7**
			D_2(GV+LA)s	0.15 ± 0.01	0.27 ± 0.02	0.03 ± 0.01	0.54 ± 0.03	-	**1+7+ 8**
			D_3(GV+LA)s	0.13 ± 0.01	0.24 ± 0.01	0.03 ± 0.01	0.33 ± 0.01	0.76 ± 0.05	**1+7-9**
			g-M_3SGVs	0.13 ± 0.01	0.24 ± 0.01	0.03 ± 0.01	0.13 ± 0.02	0.24 ± 0.05	**1+7-9**
3	B (**1+2**)	Budding, Growth, Pearling and Division	D_1(GV+LA)s	0.20 ± 0.01	0.37 ± 0.01	0.89 ± 0.03	-	**-**	**1+2+7**
			D_2(GV+LA)s	0.16 ± 0.02	0.28 ± 0.03	0.08 ± 0.02	0.65 ± 0.03	**-**	**1+2+7+8**
			g-M_2SGVs	0.19 ± 0.01	0.35 ± 0.02	0.03 ± 0.01	0.35 ± 0.03	**-**	**1+2+7+8**
4	C (**1-4**)[f]	Budding, Growth, Pearling and Division	D_1(GV+LA)s	0.11 ± 0.01	0.20 ± 0.01	0.99 ± 0.03	-	**-**	**1-4+7**
			D_2(GV+LA)s	0.34 ± 0.02	0.62 ± 0.03	0.008 ± 0.001	0.57 ± 0.03	**-**	**1-4+7+8**
			g-M_2SGVs	0.10 ± 0.01	0.18 ± 0.02	0.002 ± 0.001	0.43 ± 0.03	**-**	**1-4+7+8**
Inverted feeding order						1st feeding	2nd feeding		
Entry	g-M_0SGVs[a]	Microscopic observations[b]	Vesicles product	PL conc. [c,d]	PL_{found} / $PL_{initial}$	**8** $_{found}$/**8** $_{fed}$ [d],[e]	**7** $_{found}$/**7** $_{fed}$ [d],[e]		Final composition
5	A^+ (**1**)	Budding, Growth, Pearling and Division	D_1(GV+LA)s	0.20 ± 0.02	0.37 ± 0.04	0.43 ± 0.01	-	**-**	**1+8**
			D_2(GV+LA)s	0.18 ± 0.02	0.33 ± 0.04	0.45 ± 0.02	0.95 ± 0.01	**-**	**1+8+7**
			g-M_2SGVs	0.17 ± 0.02	0.30 ± 0.03	0.12 ± 0.01	0.05 ± 0.01	**-**	**1+8+7**
Other feedings									
Entry	g-M_0SGVs[a]	Fed with	Vesicles product						Final composition
6	A (**1**)	**10**	None/aggregates						-
7	A (**1**)	**11**	None/aggregates						-
8	A (**1**)	**12**	None/aggregates						-

[a] **1**=POPC, **2**=POPA; **3**=DOPC, **4**=DOPA, **7**=oleic acid, **8**=myristic acid, **9**=myristoleic acid; [b] Descriptions and images of the phenomena are available in the supporting information; [c] Concentrations of phospholipids **1, 2, 3** and **4** measured by Stewart assay and normalized to 0.55 mM; [d] Mean values and standard errors were determined from experiments performed in triplicates (n=3).[e] Concentration of fatty acids **7**, **8** and **9** measured by HPLC and normalized to 1 mM; [f] Analysis of the lipid boundaries containing soybean and egg-yolk extracts (Table S1, entries 5 and 6, D and E types, respectively) was not performed. C type MSGVs can be considered as a simplified model of D and E type coatings.

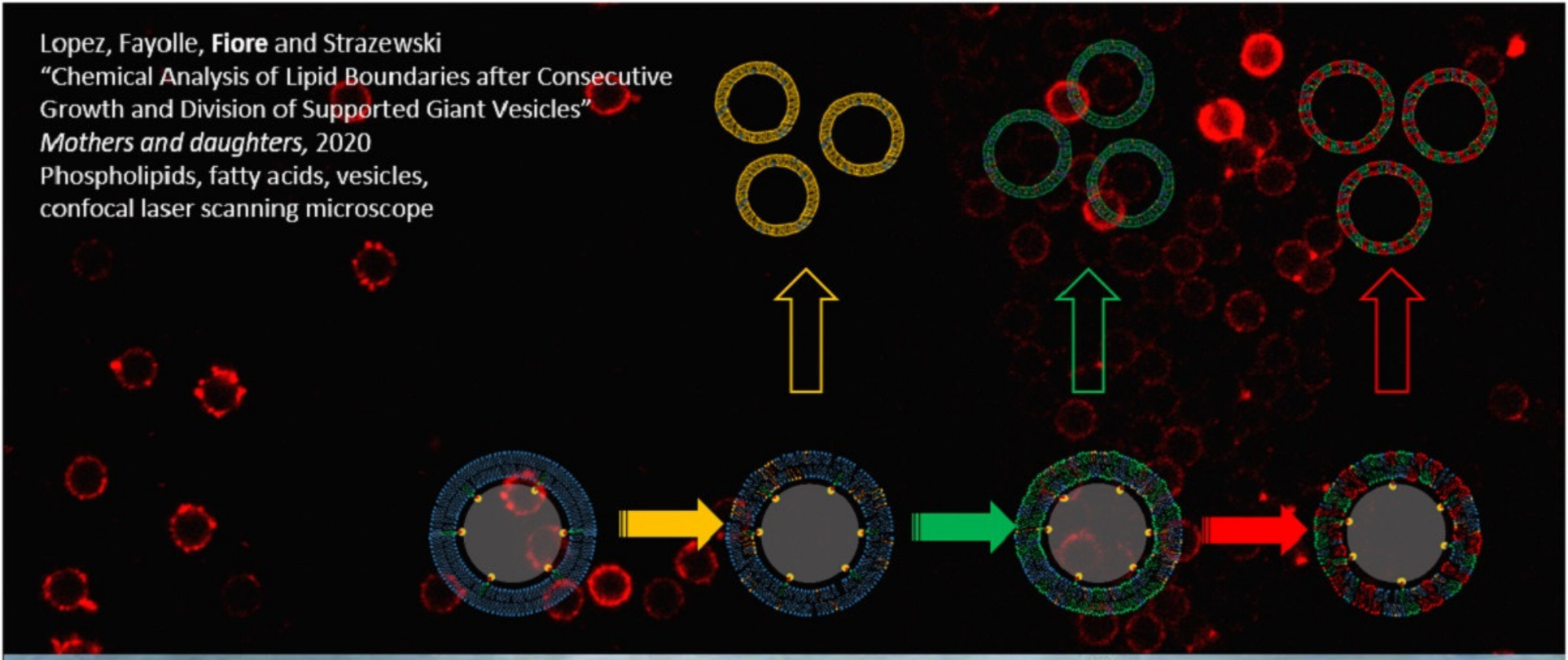
Lopez, Fayolle, **Fiore** and Strazewski
"Chemical Analysis of Lipid Boundaries after Consecutive Growth and Division of Supported Giant Vesicles"
Mothers and daughters, 2020
Phospholipids, fatty acids, vesicles,
confocal laser scanning microscope


Markey Robinson
1918 – 1999
"Mother and daughter"
Oil on canvas